ACKNOWLEDGMENTS

Dr. François Bénard's support was provided by the Medical Research Council of Canada under the Clinician-Scientist Program.

REFERENCES

1. Pearse AGE. The neuroendocrine (APUD) cells of the skin. *Am J Dermatopathol* 1980;2:121–123.
2. Yiengpruksawan A, Cort DG, Thaler HT, Urmacher C, Knapper WK. Merkel cell carcinoma. Prognosis and management. *Arch Surg* 1991;126:1514–1519.
3. Haag ML, Galss LF, Fenske NA. Merkel cell carcinoma. Diagnosis and treatment. *Dermatol Surg* 1995;21:669–683.
4. Fraker DL, Alexander HR. Isolated limb perfusion with high-dose tumor necrosis factor for extremity melanoma and sarcoma. In: DeVita VT, Hellman S, Rosenberg SA, eds. *Important Advances in Oncology 1994*. Philadelphia: JB Lippincott; 1994: 179–192.
5. Karp JS, Muehllehner DA, Mankoff DA, et al. Continuous slice PENN-PET:a positron tomography with volume imaging capability. *J Nucl Med* 1990;31:617–627.
6. Smith R, Karp J, Muehllehner G, Gualtieri E, Benard F. Singles transmission scans performed post-injection for quantitative whole body PET imaging. *IEEE Trans Nucl Sci* 1997;44:1329–1335.
7. Benard F, Smith RJ, Karp JS, Ozdemir S, Alavi A. Improved image quality of whole-body FDG PET scans by employing a practical algorithm: expectation maximization with ordered subsets [Abstract]. *J Nucl Med* 1996;37:130P.
8. Hitchcock CL, Bland KI, Laney RG III, et al. Neuroendocrine (Merkel cell) carcinoma of the skin. Its natural history, diagnosis and treatment. *Ann Surg* 1982;70:485–489.
9. Alavi JB, Alavi A, Chawluk J, et al. Positron emission tomography in patients with glioma. A predictor of prognosis. *Cancer* 1988;62:1074–1078.
10. Borbely K, Fulham MJ, Brooks RA, Di Chiro G. PET-fluorodeoxyglucose of cranial and spinal neuromas. *J Nucl Med* 1992;33:1931–1934.
11. Brown RS, Leung JY, Fisher SJ, Frey KA, Ethier SP, Wahl RL. Intratumoral distribution of tritiated fluorodeoxyglucose in breast carcinoma: I. Are inflammatory cells important? *J Nucl Med* 1995;36:1854–1861.
12. Duhaylongsod FG, Lowe VJ, Patz EF Jr, Vaughn AL, Coleman RE, Wolfe WG. Detection of primary and recurrent lung cancer by means of fluorine-18-fluorodeoxyglucose positron emission tomography (FDG PET). *J Thorac Cardiovasc Surg* 1995;110:130–140.
13. Gritters LS, Francis IR, Zasadny KR, Wahl RL. Initial assessment of PET using 2-fluorine-18-fluoro-2-deoxy-D-glucose in the imaging of malignant melanoma. *J Nucl Med* 1993;34:1420–1427.
14. Haberkorn U, Strauss LG, Dimitrakopoulou A, et al. Fluorodeoxyglucose imaging of advanced head and neck cancer after chemotherapy. *J Nucl Med* 1993;34:12–17.
15. Ito K, Kato T, Tadokoro M, et al. Recurrent rectal cancer and scar: differentiation with PET and MR imaging. *Radiology* 1992;182:549–552.
16. Karlan BY, Hawkins R, Hoh C, et al. Whole-body positron emission tomography with 2-[^{18}F]-fluoro-2-deoxy-D-glucose can detect recurrent ovarian carcinoma. *Gynecol Oncol* 1993;51:175–181.
17. Zanzonico PB, Bigler RE, Leonard RW, et al. The enzymatic basis of biodistribution of FDG: implications for tumor imaging [Abstract]. *J Nucl Med* 1985;26:64P.
18. Hawkins RA, Choi Y, Huang S-C, Messa C, Hoh CK, Phelps ME. Quantitating tumor glucose metabolism with FDG and PET. *J Nucl Med* 1992;33:339–343.
19. Alstrom H, Eriksson B, Bergstrom M, et al. Pancreatic neuroendocrine tumors: diagnosis with PET. *Radiology* 1995;195:333–337.
20. Eriksson B, Bergdtrom M, Lilja A, Ahlstrom H, Langstrom B, Ober K. Positron emission tomography (PET) in neuroendocrine gastrointestinal tumors. *Acta Oncologica* 1993;32:189–196.
21. Shulkin BL, Koeppe RA, Francis IR, Deeb GM, Lloyd RV, Thompson NW. Pheochromocytomas that do not accumulate metaiodobenzylguanidine: localization with PET and administration of FDG. *Radiology* 1993;186:711–715.
22. Shulkin BL, Wieland DM, Schwaiger M, et al. PET scanning with hydroxyephedrine: an approach to the localization of pheochromocytoma. *J Nucl Med* 1992;33:1125–1131.
23. Kwekkeboom DJ, Hoff AM, Lamberts SWJ, Oei HY, Krenning EP. Somatostatin analogue scintigraphy. A simple and sensitive method for the in vivo visualization of Merkel cell tumors and their metastases. *Arch Dermatol* 1992;128:818–821.
24. Choe W, Housini I, Mello AM. Lymphoscintigraphy in a case of Merkel cell tumor. *Clin Nucl Med* 1995;20:922–924.
25. Castagnoli A, Biti G, De Cristofaro MTR, Ferri P, Magrini SM. Merkel cell carcinoma and iodine-131-metaiodobenzylguanidine scan. *Eur J Nucl Med* 1992;19:913–916.
26. De Geeter F, Saelens E. Merkel cell carcinoma [Letter]. *Eur J Nucl Med* 1994;21:86.
27. Von Moll L, Mc Ewan AJ, Shapiro B, et al. Iodine-131-MIBG scintigraphy of neuroendocrine tumors other than pheochromocytoma and neuroblastoma. *J Nucl Med* 1987;28:978–988.
28. Wahl RL, Zasandy K, Helvie M, Hutchins GD, Weber B, Cody R. Metabolic monitoring of breast cancer chemohormonotherapy using positron emission tomography: initial evaluation. *J Clin Oncol* 1993;11:2101–2111.
29. Kubota K, Ishiwata K, Kubota R, et al. Tracer feasibility for monitoring tumor radiotherapy: a quadruple tracer study with fluorine-18-fluorodeoxyglucose or fluorine-18-fluorodeoxyuridine, L-[Methyl-^{14}C]Methionine, [6-^{3}H]Thymidine, and Gallium-67. *J Nucl Med* 1991;32:2118–2123.
30. Jansson T, Westlin JE, Ahlstrom H, Lilja A, Langstrom B, Bergh J. Positron emission tomography studies in patients with locally advanced and/or metastatic breast cancer: a method for early therapy evaluation? *J Clin Oncol* 1995;13:1470–1477.
31. Van Ginkel RJ, Hoekstra HJ, Pruim J, et al. FDG PET to evaluate response to hyperthermic isolated limb perfusion for locally advanced soft-tissue sarcoma. *J Nucl Med* 1996;37:984–990.
32. Gollub MJ, Gruen DR, Dershaw DD. Merkel cell carcinoma: CT findings in 12 patients. *AJR* 1996;167:617–620.

Response to Treatment with Yttrium 90-DOTA-Lanreotide of a Patient with Metastatic Gastrinoma

Maria Leimer, Amir Kurtaran, Peter Smith-Jones, Markus Raderer, Ernst Havlik, Peter Angelberger, Friedrich Vorbeck, Bruno Niederle, Christian Herold and Irene Virgolini

Departments of Nuclear Medicine, Oncology, Biomedical Engineering and Physics, Radiology, and Surgery, University of Vienna; and the Department of Radiochemistry, Research Center Seibersdorf, Austria

1,4,7,10-tetraazacyclododecane-N,N',N'',N'''-tetraacetic acid (DOTA)-lanreotide is a universal somatostatin (SST) receptor subtype ligand that binds to a large variety of human tumors. We report the case of a patient with metastatic gastrinoma who was treated with ^{90}Y-DOTA-lanreotide. Before treatment, dosimetry with ^{111}In-DOTA-lanreotide (150 MBq, 10 nmol) indicated a dose of 5.8 mGy/MBq for the recurrent abdominal gastrinoma, and a mean dose of ≈1.0 mGy/MBq for liver metastases (i.e., 56 and ≈10 mGy/MBq for ^{90}Y-DOTA-lanreotide, respectively). After four infusions of ^{90}Y-DOTA-lanreotide (each 1 GBq, ≈30 nmol) over a 6-mo period, the ^{111}In-DOTA-lanreotide scintigraphy of the liver had returned to a nearly normal condition and a remarkably decreased uptake by the recurrent gastrinoma was calculated (≈5 mGy/MBq for ^{90}Y-DOTA-lanreotide). The imaging results were well-correlated with a 25% regression of the liver metastases as indicated by CT. Blood, urine and whole-body clearances of ^{111}In-DOTA-lanreotide and ^{90}Y-DOTA-lanreotide were very similar. The DOTA-lanreotide promises to be useful for functional tumor diagnosis (^{111}In-DOTA-lanreotide) and receptor-mediated tumor radiotherapy (^{90}Y-DOTA-lanreotide).

Key Words: DOTA-lanreotide; somatostatin receptor; tumor radiotherapy; gastrinoma

J Nucl Med 1998; 39:2090–2094

The overexpression of peptide receptors (R) on human tumor cells compared with normal tissues and cells has provided the basis for the successful use of radiolabeled somatostatin (SST) analogs for tumor targeting (*1–3*). Some peptide tracers have

Received Feb. 3, 1998; revision accepted Jul. 6, 1998.

For correspondence or reprints contact: Irene Virgolini, MD, Department of Nuclear Medicine, University of Vienna, Währinger Gürtel 18–20, Ebene 3L, A-1090 Vienna, Austria.

been shown to be effective not only in the diagnosing and staging of tumors and their metastases, but also in the initial efforts implemented for these peptides to prove the concept of receptor-mediated radiotherapy by using large amounts of the diagnostic compound ^{111}In-diethylenetriamine pentaacetic acid-D-Phe^{1}-octreotide (OCT) (*3*).

Recently, we have developed the novel hSSTR-recognizing ligand 1,4,7,10-tetraazacyclododecane-N,N′,N″,N‴-tetraacetic acid (DOTA)-lanreotide (*4*). This compound binds to all known hSSTR as well as to a variety of primary and immortalized tumor cells (*4*), which have been shown to express one or the other hSSTR subtype (*5*). Scintigraphy with ^{111}In-DOTA-lanreotide has already indicated a high tumor accumulation (i.e., 0.4–5 mGy/MBq) of this novel agent in patients with different tumor types (*6*). In particular, in patients with neuroendocrine tumors, the tumor accumulation of ^{111}In-DOTA-lanreotide was significantly higher compared with ^{111}In-OCT (*6–8*). Furthermore, as opposed to experimental radionuclide therapy with monoclonal antibodies that have already entered the clinic, the radiolabeled DOTA-lanreotide peptide is not only well-defined with respect to its specific receptor-binding properties (*4*), but it also clears rapidly from circulation after intravenous injection (*6*). Here we report on the first radiotherapy performed with ^{90}Y-DOTA-lanreotide in a patient with metastatic gastrinoma.

CASE REPORT AND RESULTS

In 1987, a 48-yr-old man had surgery performed on an acute abdomen that had evolved by perforation of an atypical ulcer of the duodenojejunal flexure. Despite postsurgical inconspicuous gastroscopy, the patient suffered from recurring periods of epigastric pain. The pain was resistant to antacids and histamine receptor-blocking agents. In 1989, a peptic gastric ulcer was detected, and because of the rise in plasma gastrin (370 pg/ml, normal 25–115 pg/ml) and the pathological secretin test (after 5 min, 1400 pg/ml), Zollinger-Ellison syndrome was diagnosed. An abdominal CT showed a tumor in the pancreatic head. The tumor, measuring 2 cm in diameter, was then enucleated from the uncinate process and all visible lymph nodes were extirpated. Pathohistology indicated a malignant gastrin and pancreatic polypeptide-producing islet cell tumor with two lymph node metastases. The multiple endocrine neoplasia syndrome 1 was excluded biochemically. Follow-up examinations were normal until 1994.

In July 1995, an increased gastrin level (66,000 pg/ml) was measured. CT of the abdomen revealed two liver metastases (approximately 3 cm in diameter) in segments VII and VIII and recurrence of the gastrinoma dorsal of the pancreatic head (2 cm in diameter). The patient was free of clinical symptoms under therapy with proton pump inhibitors and refused any further intervention.

In May 1997, the liver metastases had increased to more than seven large, highly vascularized formations in segments IV, V, VII and VIII and measured up to 3 cm in diameter. Despite remarkably elevated serum gastrin values, very high serum triglyceride levels were measured during the whole course of the disease (up to 1780 mg/dl). Gastrin values were 86,000 pg/ml in April 1996, increased to 120,000 pg/ml in December 1996 and remained persistently high thereafter.

Because of the extrahepatic tumor mass, experimental radiotherapy with ^{90}Y-DOTA-lanreotide as an alternative therapeutic approach to embolization was considered. The patient was referred for evaluation of the tumor dosage using ^{111}In-DOTA-lanreotide dosimetry as described by Virgolini et al. (*6*). The application of ^{111}In-DOTA-lanreotide for diagnostic scintigraphy, as well as of ^{90}Y-DOTA-lanreotide for radiotherapy to patients, was approved by the Ethical Committee of the Medical Faculty of the University of Vienna. Synthesis and radiolabeling of DOTA-lanreotide are described by Smith-Jones et al. (*4*) and Virgolini et al. (*6*). The dosimetry protocol included whole-body gamma camera imaging as well as blood, urine and feces collections over 72 hr and is detailed by Virgolini et al. (*6*). The specific activity was 20 MBq/nmol ^{111}In-DOTA-lanreotide and 40 MBq/nmol ^{90}Y-DOTA-lanreotide.

Indium-111-DOTA-lanreotide was administered as a single intravenous bolus injection in 3 ml 0.9% NaCl solution (150 MBq, 10 nmol peptide). Planar and SPECT acquisitions were performed with a Picker PRISM 1000 gamma camera (Picker, Bedford Heights, OH) equipped with a medium energy collimator. At the time of ^{111}In-DOTA-lanreotide injection, the field of view covered the upper abdomen. The radiation of both photopeaks (173 keV and 247 keV) with settings of windows at 20% were used. Sequential images were recorded over 30 min (matrix 128 × 128 pixels). Serial whole-body acquisitions were then recorded in anterior and posterior views (matrix 256 × 1024, 15 min each) at 0.5, 3, 6, 24, 48 and 72 hr postinjection. SPECT was performed in a 360° circle in 6° steps, 30 sec per step. SPECT data were reconstructed using a LOP filter (cutoff frequency 10%) and postfiltered using a ramp filter (slice thickness, 4 mm). For calculation of the tumor and organ dosages, regions of interest (ROIs) were drawn on every whole-body scintigram at each time point. The mean of the anterior and posterior counts was calculated for ROIs of the recurrent abdominal gastrinoma, three liver metastases, normal liver, spleen, kidneys and urinary bladder, as well as of background regions, using the software written for the Picker analyzing system. Organ dose calculation was performed on the basis of the MIRD (Medical Internal Radiation Dose) concept (*9*). The anteroposterior and posteroanterior ROI counts were added and the background activity subtracted. The data were subjected to decay correlation back to the time of injection and expressed as percentage injected dose based on the initial whole-body scan (i.e., 100%). Time-activity curves were then constructed and the biological half-lives and initial accumulation estimated. These data were used to determine the residence time for radioactivity in tumors, various organs and the whole body. CT tumor volume was calculated by measuring the extensions of the largest lesions in three planes (Phillips SR7000 spiral CT [Phillips Medical System International, BV Eindoven, the Netherlands], 10-mm slice thickness, 10-mm table speed, 5-mm reconstruction).

Significant accumulations of ^{111}In-DOTA-lanreotide were in the liver metastases and also in the recurrent abdominal tumor mass (Fig. 1A). The calculated tumor dose amounted to 5.8 mGy/MBq for the recurrent gastrinoma and ranged between 0.44 and 1.95 mGy/MBq for the liver metastases. The doses to the kidneys, spleen, liver, urinary bladder and the bone marrow as well as the effective dose are depicted in Table 1.

On the basis of the high tumor accumulation, radiotherapy with ^{90}Y-DOTA-lanreotide was initiated in June 1997. An 1 GBq dose of ^{90}Y-DOTA-lanreotide (30 nmol peptide) was infused intravenously in 500 ml 0.9% saline solution over 0.5 hr. Blood and urinary samples were gathered over 72 hr postinjection. Whole-body measurements were also performed by counting the Bremsstrahlung radiation with a whole-body scanner. Application of the labeled peptide was well tolerated without any subjective side effects. However, an effect on peripheral blood cells was observed within the 24-hr postinfusion period (Grade 1 toxicity according to World Health Organization standard criteria, i.e., leukocytes dropped from 6.4 G/liter to 3.7 G/liter and erythrocytes from 4.2 T/liter to 3.5 T/liter), but had normalized at 3 days after infusion, and then remained stable. The differential blood count revealed the presence of lymphocytopenia (0.8 G/liter), whereas the other leukocyte subpopulations were not affected (neutrophils 2.6 G/liter, monocytes 0.1 G/liter, eosinophils 0.1 G/liter). The compara-

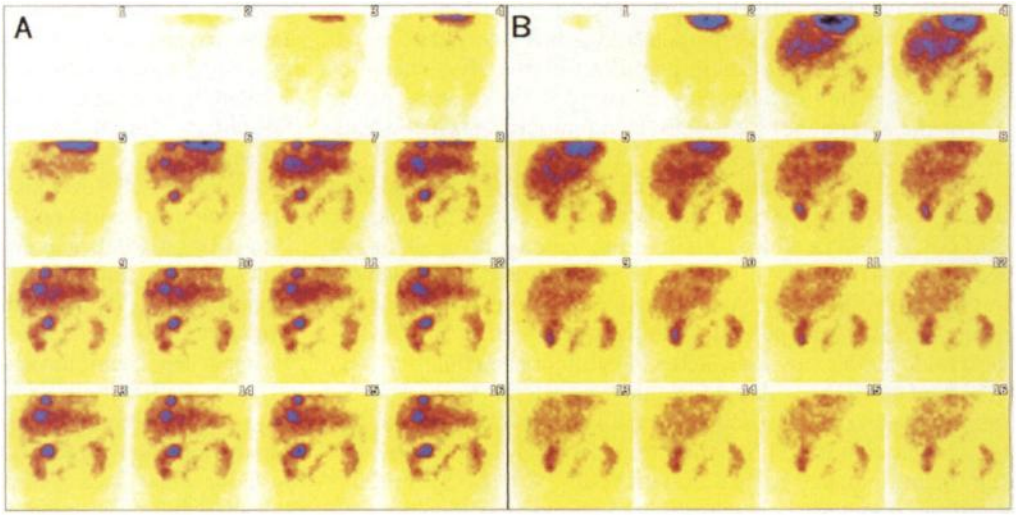

FIGURE 1. Sequential anterior study of ^{111}In-DOTA-lanreotide (~150 MBq) before (A) and after (B) four cycles of treatment with ^{90}Y-DOTA. Time span between both scintigraphs was 6 mo.

tive blood clearances (Fig. 2) and urinary clearances (Fig. 3) for ^{111}In- and ^{90}Y-DOTA-lanreotide in this patient were comparable up to 72 hr postinjection.

Another dose of ^{90}Y-DOTA-lanreotide (1 GBq) was administered in July 1997. CT follow-up in August 1997 indicated a stable tumor disease. A second dosimetry study with ^{111}In-DOTA-lanreotide was performed in September 1997. Compared with the first dosimetry study, a slightly decreasing tumor dose was calculated for all tumor lesions (Table 1). Another two treatment doses of ^{90}Y-DOTA-lanreotide, each 1 GBq, were administered in September and October 1997. Also, these two treatments were well tolerated by the patient, and again a clinically insignificant drop in the peripheral leukocyte cell count was observed during the first 24-hr postinjection period, reaching initial values within 3 days.

In November 1997 a third diagnostic scintigraphy study with ^{111}In-DOTA-lanreotide was performed. During sequential scanning, no tumor uptake could be identified with certainty (Fig. 1B). The SPECT study disclosed the presence of the abdominal recurrent tumor in the area of the pancreatic head and heterogeneous liver uptake, but no focal liver accumulation, as visualized before the first treatment cycle. By dosimetry obtained from ROIs identical to those applied for the first and second ^{111}In-DOTA-lanreotide whole-body scans, a dose of ≈0.5 mGy/MBq was calculated for the abdominal gastrinoma. However, the calculable dose for the liver metastases was ≈0.15 mGy/MBq and was similar to the dose calculated for the normal liver (0.1 mGy/MBq). Furthermore, the doses for the spleen, kidneys, urinary bladder and bone marrow were similar to those before treatment. The effective dose determined for the third ^{111}In-DOTA-lanreotide scintigraphy study was slightly reduced and reflected a faster whole-body clearance of radioactivity.

CT results from November 1997 indicated a decrease in overall tumor mass (25%), along with marked necrotic changes and devascularization of most liver lesions (Fig. 4). For the three largest liver metastases, the following tumor volume was calculated: liver metastasis 1 decreased from 70.3 mm^3 (on 5/22/97) to 49.2 mm^3 (on 11/20/97), liver metastasis 2 decreased from 58.3 mm^3 (5/22/97) to 42.3 mm^3 (11/20/97) and liver metastasis 3 decreased from 5.5 mm^3 (5/22/97) to 4.1 mm^3 (11/20/97).

The patient reported an improved quality of life and weight gain of 4 kg. Despite the clinical improvement, the gastrin levels in January 1998 were 86,000 pg/ml, along with persistently excessive hypertriglyceridemia (>700 mg/dl).

DISCUSSION

This is the first report of the therapeutic application of ^{90}Y-DOTA-lanreotide in a patient who had advanced gastrinoma. After four treatment cycles with ^{90}Y-DOTA-lanreotide, liver metastases had remarkably decreased and the patient's quality of life improved.

The concept of peptide receptor-mediated radiotherapy is a novel approach to anticancer treatment, and there is only limited information concerning its use in clinical oncology. Promising preliminary data have been obtained with high doses of ^{111}In-OCT in patients with neuroendocrine tumors and lymphomas (*3*). The capability of ^{111}In-DOTA-lanreotide to visualize

TABLE 1
Organ Doses Calculated From ^{111}In-DOTA-Lanreotide Scintigraphy

Organ	First dosimetry 4/22/97		Second dosimetry 9/16/97		Third dosimetry 11/18/97	
	^{111}In	^{90}Y	^{111}In	^{90}Y	^{111}In	^{90}Y
Recurrent gastrinoma	5.80	56	3.6	58	≈0.5	≈5
Liver metastasis 1	0.44	4.2	0.39	4.7	≈0.15	≈1
Liver metastasis 2	0.62	5.8	0.38	4.6	≈0.17	≈1.5
Liver metastasis 3	1.95	18.8	0.76	10.8	n.c.	n.c.
Kidneys	0.25	2.43	0.21	2.00	0.21	1.98
Liver	0.11	0.59	0.11	0.62	0.10	0.57
Spleen	0.28	2.65	0.32	3.35	0.23	1.68
Urinary bladder	0.18	1.42	0.18	1.41	6.17	1.42
Bone marrow	0.07	0.29	0.06	0.29	0.05	0.25
Effective dose	0.09	0.49	0.09	0.51	0.08	0.44

All values are given in mGy/MBq; n.c. = not calculable due to poor tumor-to-background ratio.

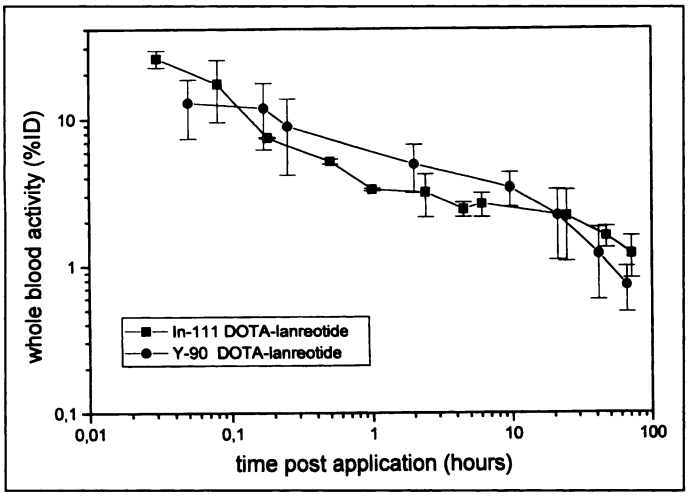

FIGURE 2. Comparative blood kinetics of ^{111}In-DOTA-lanreotide (150 MBq, n = 3) and ^{90}Y-DOTA-lanreotide (~1 GBq, n = 4).

tumors of neuroendocrine origin, as well as adenocarcinomas and lymphomas, has already been outlined, along with biodistribution, safety and tumor doses (*6*). On the basis of the biodistribution data of ^{111}In-DOTA-lanreotide and the resultant predicted dosimetry of ^{90}Y-DOTA-lanreotide, we applied the radiotherapeutic agent to this patient with gastrinoma.

This case shows that ^{111}In-DOTA-lanreotide and ^{90}Y-DOTA-lanreotide have very similar blood, urine and whole-body clearance rates. The comparative blood clearances for ^{111}In- and ^{90}Y-DOTA-lanreotide in this patient were initially different because of the different mode of application (bolus injection versus infusion over 0.5 hr), but at later time points (>15 min), they were comparable (Fig. 2). Also, a comparable urinary clearance was observed for ^{111}In- and ^{90}Y-DOTA-lanreotide (Fig. 3). Furthermore, previous studies have shown that both tracers also exhibit an identical in vitro binding behavior (*4*). These observations altogether provide the basis for using ^{111}In-DOTA-lanreotide to monitor tumor patients undergoing treatment with ^{90}Y-DOTA-lanreotide.

Whereas, after two treatment cycles with ^{90}Y-DOTA-lanreotide (cumulative dose, 2 GBq), a stable disease was observed by CT and measurable tumor response was demonstrable after four treatment cycles (cumulative dose, 4 GBq). The treatment effect could be seen by repeated scintigraphy showing decreased accumulation of ^{111}In-DOTA-lanreotide. This imaging result can be interpreted on the basis of tumor cell necrosis after treatment, after a cumulative tumor radiation dose of 25–200 Gy given over a 6-mo period. The possibility of down-regulation of SSTR expression on the tumor cells seems unlikely because the peptide doses applied were very low, and the time span between treatments and scintigraphs was approximately 1 mo. Furthermore, the selective killing of SSTR-positive cells within the tumor mass is unlikely because of the long beta range of ^{90}Y-DOTA-lanreotide and the homogeneous radiation dose distribution (*9*). Because of the overall reduction of the tumor size after the treatment cycles with ^{90}Y-DOTA-lanreotide, growth of SSTR-negative cell population also seems unlikely. The 24-hr drop in leukocytes is unusual when compared with ^{90}Y-labeled antibodies used for treatment, which normally results in a delayed bone marrow depression (*10*). However, in this patient an effect was only observed on the lymphocyte subpopulation, while the other subtypes remained within normal range. Therefore, one cannot rule out direct interaction between our ^{90}Y-labeled substance and SSTR-expressing circulating lymphocytes (*11*).

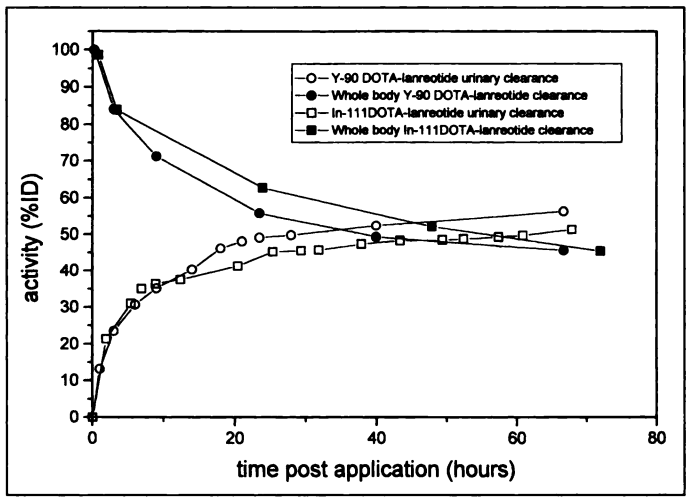

FIGURE 3. Comparative urinary excretion and whole-body clearance of ^{111}In-DOTA-lanreotide (150 MBq) and ^{90}Y-DOTA-lanreotide (~1 GBq).

Gastroenteropancreatic tumors exhibit functional features connected to regulatory and secretory events in the enterochromaffin-like cells present in these malignancies (*12*). Significant formation of hormonally active peptides, including gastrin, occurs in carcinomas derived from these cells. Hypersecretion of gastrin in enterochromaffin-like cells can be inhibited by SST and its long-acting analogs (*13,14*). One also would have expected a biochemical response to ^{90}Y-DOTA-lanreotide treatment in this patient with gastrinoma. However, tremendously increased serum gastrin values were found during the course of the disease, which were still highly elevated after the fourth treatment cycle. This again may be associated with tumor cell necrosis and increased gastrin secretion from damaged tumor cells (*15*) and indicates the presence of hormonally active disease. We believe that in this patient the gastrin values are not representative because of excessive hypertriglyceridemia. The possible effects of triglycerides on gastrin release in animal studies have been discussed previously (*16*). The gastrin values measured in this patient (dilution series) were proportional to the triglyceride values and were therefore regarded not to be reliable to demonstrate tumor response (a regression analysis indicated $r = 0.58$ and $p = 0.034$ between serum gastrin and triglycerides values).

Although gastrinomas are usually characterized by slow growth, curative treatment is difficult in patients with metastatic disease (*17*). Surgical and medical interventions proved to have low curative rates, however, may palliatively improve the clinical symptoms. This case now presents a new therapeutic approach for the clinical management of patients with metastasized SSTR-expressing gastrinomas. However, a variety of questions concerning the experimental peptide receptor radiotherapy using ^{90}Y-DOTA-lanreotide or other SSTR analogs cannot be answered at the present time. A greater number of studies is warranted to further evaluate the optimal dose regimen, treatment duration, monitoring process or concomitant treatment possibilities.

CONCLUSION

We conclude that receptor-mediated radiotherapy using the novel SSTR tracer ^{90}Y-DOTA-lanreotide may present an alternative approach for the treatment of advanced SSTR-expressing tumors. Repeated scintigraphies using ^{111}In-DOTA-lanreotide may be used to monitor the response of the disease toward treatment with the radioligand.

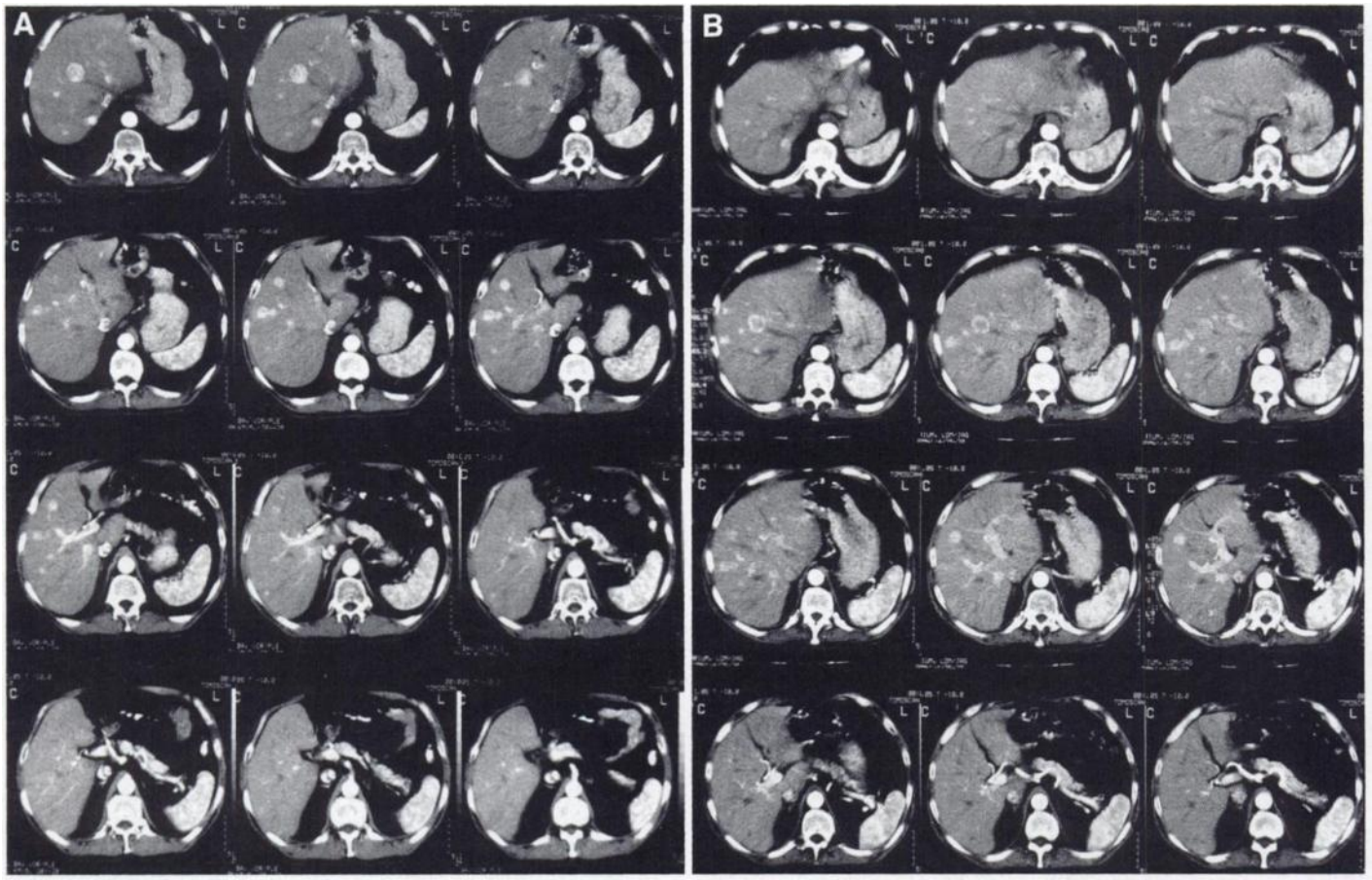

FIGURE 4. CT of liver and abdomen before (A) and after (B) four treatment cycles with ^{90}Y-DOTA-lanreotide.

ACKNOWLEDGMENTS

We thank our nurses at the Department of Nuclear Medicine, University of Vienna. We are indebted to Drs. R. Dudczak, K. Kletter, S. Shene, H. Sinzinger and K. Weiss, Department of Nuclear Medicine, for organizational help.

REFERENCES

1. Lamberts SWJ, Bakker WH, Reubi JC, Krenning EP. Somatostatin receptor imaging in the localization of endocrine tumors. *N Engl J Med* 1990;323:1246–1249.
2. Virgolini I, Angelberger P, Li S, et al. In vitro and in vivo studies of three radiolabelled somatostatin analogues: ^{123}I-octreotide (OCT), ^{123}I-Tyr-3-OCT and ^{111}In-DTPA-D-Phe-1-OCT. *Eur J Nucl Med* 1996;23:1388–1399.
3. Krenning EP, Kooij PP, Bakker WH, et al. Radiotherapy with a radiolabeled somatostatin analogue, ^{111}In-DTPA-D-Phe1-octreotide. *Ann N Y Acad Sci* 1994;733:496–506.
4. Smith-Jones P, Bischof C, Leimer M, et al. "MAURITIUS" a novel somatostatin analog for tumor diagnosis and therapy [Abstract]. *J Nucl Med* 1998;39:223P.
5. Virgolini I, Pangerl T, Bischof C, Smith-Jones P, Peck-Radosavljevic M. Somatostatin receptor subtype expression in human tissues: a prediction for diagnosis and treatment of cancer? *Eur J Clin Invest* 1997;27:645–647.
6. Virgolini I, Szilvasi I, Kurtaran A, et al. Indium-111-DOTA-lanreotide: biodistribution, safety and radiation absorbed dose in tumor patients. *J Nucl Med* 1998;39:1928–1936.
7. Krenning EP, Kooij PPM, Pauwels S, et al. Somatostatin receptor: scintigraphy and radionuclide therapy. *Digestion* 1996;57(suppl):57–61.
8. Anderson CJ, Pajeaun TS, Edwards WB, Sherman ELC, Rogers BE, Welch MJ. In vitro and in vivo evaluation of copper-64 octreotide conjugates. *J Nucl Med* 1995;36:2315–2325.
9. Loevinger R, Budinger T, Watson E. *MIRD primer for absorbed dose calculations.* Reston, VA: Society of Nuclear Medicine; 1988.
10. Herpst JM, Klein JL, Leichner PK, Quadri SM, Vriesendorp HM. Survival of patients with resistant Hodgkin's disease after polyclonal yttrium 90-labeled antiferritin treatment. *J Clin Oncol* 1995;13:2394–2400.
11. Hiruma K, Koike T, Nakamura H, et al. Somatostatin receptors on human lymphocytes and leukaemia cells. *Immunology* 1990;71:480–485.
12. Modlin IM, Tang LH. The gastric enterochromaffin-like cell: an enigmatic cellular link. *Gastroenterology* 1996;111:783–810.
13. Kvols LK. Somatostatin-receptor imaging of human malignancies: a new era in the localization, staging, and treatment of tumors. *Gastroenterology* 1993;105:1909–1914.
14. Eriksson B, Janson ET, Bax ND, et al. The use of new somatostatin analogs, lanreotide and octastatin, in neuroendocrine gastrointestinal tumours. *Digestion* 1996;1(suppl): 77–80.
15. Beales IL, Post L, Calam J, Yamada T, Delvalle J. Tumour necrosis factor alpha stimulates gastrin release from canine and human antral G cells: possible mechanism of the *Helicobacter pylori*-gastrin link. *Eur J Clin Invest* 1996;26:609–611.
16. Shiratori K, Watanabe S, Takeuchi T. Intestinal fat digestion plays a significant role in fat-induced suppression of gastric acid secretion and gastrin release in the rat. *Dig Dis Sci* 1993;38:2267–2672.
17. Modlin IM, Lewis JJ, Ahlman H, Bilchik AJ, Kumar RR. Management of unresectable malignant endocrine tumors of the pancreas. *Surgery* 1993;176:507–518.